JCTC Journal of Chemical Theory and Computation

LETTER

pubs.acs.org/JCTC

NH_4^+ Resides Inside the Water 20-mer Cage As Opposed to H_3O^+, Which Resides on the Surface: A First Principles Molecular Dynamics Simulation Study

Soohaeng Yoo Willow, N. Jiten Singh,* and Kwang S. Kim*

Center for Superfunctional Materials, Department of Chemistry, Pohang University of Science and Technology, San 31, Hyojadong, Namgu, Pohang 790-784, Korea

Supporting Information

ABSTRACT: Experimental vibrational predissociation spectra of the magic $NH_4^+(H_2O)_{20}$ clusters are close to those of the magic $H_3O^+(H_2O)_{20}$ clusters. It has been assumed that the geometric features of $NH_4^+(H_2O)_{20}$ clusters might be close to those of $H_3O^+(H_2O)_{20}$ clusters, in which H_3O^+ resides on the surface. Car−Parrinello molecular dynamics simulations in conjunction with density functional theory calculations are performed to generate the infrared spectra of the magic $NH_4^+(H_2O)_{20}$ clusters. In comparison with the experimental vibrational predissociation spectra of $NH_4^+(H_2O)_{20}$, we find that NH_4^+ is *inside* the cage structure of $NH_4^+(H_2O)_{20}$ as opposed to *on* the surface structure. This shows a clear distinction between the structures of $NH_4^+(H_2O)_{20}$ and $H_3O^+(H_2O)_{20}$ as well as between the hydration phenomena of NH_4^+ and H_3O^+.

INTRODUCTION

Since solvated ions play a pivotal role in the chemical and physical properties of chemical and biological systems[1,2] and in the environment of the upper atmosphere,[3] diverse experimental and theoretical approaches have been carried out to understand the intriguing phenomena of interactions between ions and solvent molecules. Useful information has been gained from studies of the solvation of cations[4−10] and anions[11−19] in the gas phase as well as water clusters.[20−28]

Solvated ammonium (NH_4^+) cations have been intensively studied experimentally[29−34] and theoretically[35−43] due to their similarity to the solvated hydronium (H_3O^+) in that both clusters have an excess proton. The similarity and difference between $H_3O^+(H_2O)_n$ and $NH_4^+(H_2O)_n$ could shed light on the intriguing role of how protonated water systems are related to proton transfer in aqueous chemistry and biology.[44−49] One interesting experimental IR spectrum of $NH_4^+(H_2O)_{4-6}$ showed the peak of NH_d stretching clearly in the range of 2900−3450 cm^{-1}, where NH_d indicates a dangling NH bond.[34,35] For theoretical interpretation of the experimental IR spectra, some low-lying structures were identified to show a dangling NH_d appearance.[39] The global minimum structures of $NH_4^+(H_2O)_{4-6}$ for the complete basis set (CBS) limit at the CCSD(T) level of theory have no dangling NH_d since NH_4^+ is fully solvated in the global minimum isomers. Hence, several low-lying structures would be required for interpretation of the experimental IR spectra.

The experimental IR spectra for larger clusters of $NH_4^+(H_2O)_n$ ($n > 8$) did not show the peak of NH_d stretching near 2900−3450 cm^{-1}.[32,34,35] Furthermore, vibrational predissociation spectra of the magic $NH_4^+(H_2O)_{20}$ clusters in 2500−3900 cm^{-1} are close to those of the magic $H_3O^+(H_2O)_{20}$ clusters. It has been assumed that the geometric features of $NH_4^+(H_2O)_{20}$ clusters might be the same as those of $H_3O^+(H_2O)_{20}$ clusters, in which H_3O^+ prefers to be on the surface of clusters. Diken et al. suggested several "handmade" structures of $NH_4^+(H_2O)_{20}$, in which the isomer with NH_4^+ on the surface of clusters was lower in internal energy than that with the fully solvated NH_4^+.[32] On the basis of their "handmade" structures, they discussed that the experimental vibrational spectra failed to display the dangled NH_d stretch near 3450 cm^{-1} since its peak might overlap with OH_d stretching transitions, where OH_d indicates a dangling OH bond of water. Since Brutschy and co-workers[8] reported the intriguing mass spectra of the magic clusters of $NH_4^+(H_2O)_{20}$, $K^+(H_2O)_{20}$, and $Cs^+(H_2O)_{20}$, we briefly addressed that, for $NH_4^+(H_2O)_{20}$, the structure with the NH_4^+ ion inside the cage is more stable than that on the surface of the cage by about 2 kcal/mol, and $K^+(H_2O)_{20}$ and $Cs^+(H_2O)_{20}$ also show internal structures.[49] Then, Douady et al.[40] studied low-lying isomers of $NH_4^+(H_2O)_n$ ($n \leq 24$). They confirmed that NH_4^+ is fully solvated in the global minimum structures for clusters $NH_4^+(H_2O)_n$ ($n \geq 6$). In addition, the isomers $NH_4^+(H_2O)_{20}$ with the fully solvated NH_4^+ were lower in internal energy by 1−4 kcal/mol than the isomers with a dangling NH_d of NH_4^+ residing on their surfaces. In this letter, we present a study of low-lying isomers of $NH_4^+(H_2O)_{20}$ and calculations of their infrared (IR) spectra to compare them with the experimental spectra.

COMPUTATIONAL APPROACH

Global Search of $NH_4^+(H_2O)_{20}$. We searched for low-lying energy structures using the density-functional tight binding theory (DFTB).[50] The basin-hopping global optimization method[51,52] was used to search for the geometries of low-lying isomers. A key idea of the basin-hopping method is to generate the transformed potential-energy surface (PES) $\tilde{U}$ using the

Received: July 12, 2011
Published: October 11, 2011

following mapping equation

$$\tilde{U}(N, \mathbf{r}_1, \mathbf{r}_2, ..., \mathbf{r}_N) = \min\{U(N, \mathbf{r}_1, \mathbf{r}_2, ..., \mathbf{r}_N)\}$$

where min denotes the energy minimization with starting configuration of $\{\mathbf{r}_1, ..., \mathbf{r}_N\}$ and U is the PES. This transformed PES $\tilde{U}$ removes the potential well existing in PES U and allows the system "hop" directly between different local minima at each step.

Since DFTB is much less reliable in determining the relative stability between isomers, the following three steps were employed to seek possible low-lying isomers: (1) The database of the top ~100 low-lying isomers from the global search with DFTB was categorized into distinct structural families according to their different pentagonal dodecahedron $(H_2O)_{20}$ clusters. Note that the low-lying isomers with the fully solvated NH_4^+ have the pentagonal dodecahedron $(H_2O)_{20}$ clusters. (2) The geometries within each different structural family furthermore were optimized using the Becke−3−Lee−Yang−Parr (B3LYP) hybrid functional[53,54] to screen the top 10 low-lying isomers. (3) Finally, the resolution of identity MP2 (RIMP2) calculations were performed for more-accurate energies and to determine the reliable low-lying isomers.[55] DFT calculations with the B3LYP hybrid functional were mainly used as a screening tool since it can yield more reliable energy rankings than DFTB. Recently, it has been reported that the dispersion interaction correction should be included into DFT to accurately predict thermochemical properties, electronic excitations, infrared vibrational spectra, and solvent effects.[56−59] Hence, we employed the M06-2X functional in order to include the corrected dispersion interactions into the potential energy calculations.[59] Thresholds of 10^{-6} au (convergence of the potential energy) and 0.001 au/bohr (convergence of the gradient) were used during the geometry optimizations. The geometry optimization and vibrational frequency calculations were carried out at the level of B3LYP/aug-cc-pVDZ′ (aVDZ′)[60,61] (in which ′ denotes that the diffuse basis function of the hydrogen atom was removed) and M06-2X/aug-cc-pVDZ (aVDZ) theories using the Gaussian 03 suite of programs.[62] TURBOMOLE[63] was used for geometry optimization at the level of RIMP2/aVDZ theory.

Simulated Infrared spectrum. We performed Car−Parrinello molecular dynamics (CP-MD) simulations[64,65] at a temperature of 125 K to generate the simulated infrared spectra. The CP-MD simulations were carried out at the level of the plane-wave-pseudopotential density functional theory with the Becke exchange[53] and Lee−Yang−Parr correlation[54] (BLYP) functionals. The core−valence interaction was described by a norm-conserving Troullier−Martins pseudopotential,[66] and the wave function energy cutoff value was 90 Ry. A fictitious electron mass of 600 au and an integration step of dt = 0.1 fs were used. A Nose−Hoover thermostat was employed to generate the canonical ensemble (constant volume and constant temperature). During the simulations of 10 ps, we kept the molecules at the center of isolated cubic boxes of side lengths L = 15 Å for $NH_4^+(H_2O)_{20}$. From the last 6 ps trajectory of the CP-MD simulations, we evaluated the time correlation function to investigate the spectra of the clusters in the equilibrium state. During NVT simulations, we monitored whether other isomers would be sampled, confirming that the hydrogen bond network of isomers remained. The Fourier transform of dipole moment autocorrelation functions was carried out. The infrared absorption spectrum can be computed from FT-DACF as

$$I(\omega) = (\hbar\beta/2\pi)\omega^2 \int \mathrm{d}t\, \mathrm{e}^{-i\omega t}\langle\mu(0)\,\mu(t)\rangle$$

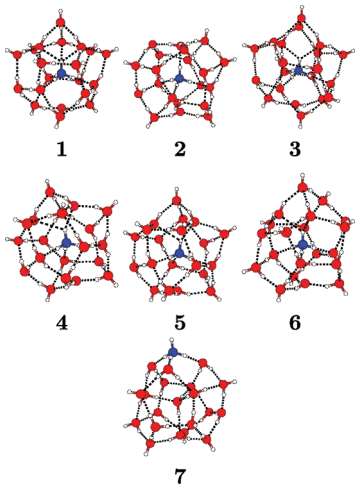

Figure 1. Possible low-lying isomers of $NH_4^+(H_2O)_{20}$ optimized at RIMP2/aVDZ. Atoms of O, N, and H are highlighted in red, blue, and white, respectively. Six isomers with the fully solvated NH_4^+ are labeled as **1**−**6**. The isomer labeled **7** has one dangling NH_d due to NH_4^+ residing on the surface.[32] Isomer **3** was suggested by Douady et al.[40]

Here, the symbols are used to denote intensity (I), frequency (ω), Plank constant ($\hbar = h/2\pi$), inverse of the Boltzmann constant multiplied by temperature ($\beta = 1/kT$), time (t), and dipole moment (μ), which is the total dipole moment of the clusters rather than the dipole moment of each molecule. For computational and interpretative purposes, it is more convenient to compute the autocorrelation function of the time derivative of the dipole moment:

$$I(\omega) = (\hbar\beta/2\pi) \int \mathrm{d}t\, \mathrm{e}^{-i\omega t}\langle\dot{\mu}(0)\,\dot{\mu}(t)\rangle$$

as discussed by Schmitt and Voth.[67] Hence, this method was employed in our calculations.

RESULTS AND DISCUSSION

Even though the basin-hopping method is a very efficient global search method, there is a limitation in searching for the global minimum structures using the basin-hopping method coupled with DFTB since the number of possible isomers of $NH_4^+(H_2O)_n$ increases dramatically with the increase of n (the number of water molecules) and DFTB is not as fast as the empirical water potentials with regard to the computational speed of the energy calculation. Since DFTB is much less reliable in determining the relative stability between isomers, we do not claim that we sampled the true global minimum energy structure of $NH_4^+(H_2O)_{20}$ within the top ~100 low-lying isomers from the global search with DFTB. Instead, we present low-lying energy structures at RIMP2/aVDZ in comparison with previously reported low-lying energy structures as the most likely candidate for the global minimum energy structure.

The selected low-lying isomers for the calculation of IR spectra are shown in Figure 1. Structures **1**−**6** are low-lying energy isomers with fully solvated NH_4^+. Isomers **1**−**6** have different pentagonal dodecahedron $(H_2O)_{20}$ clusters. Isomer **7** has NH_4^+ residing on the surface, as suggested by Diken et al.[32] Relative energies (ΔE_e and ΔE_0 in kcal/mol) of the B3LYP, M06-2X, and RIMP2 calculations are listed in Table 1. The effect of harmonic zero-point energies (ZPE) at the M06-2X/aVDZ level of theory

Table 1. Relative Energies (in kcal/mol) without (ΔE_e) and with (ΔE_0) Harmonic Zero-Point Energy (ZPE) Corrections for the Low-Lying Isomers of $NH_4^+(H_2O)_{20}$ Shown in Figure 1[a]

	B3LYP/aVDZ′		M06-2X/aVDZ		RIMP2/aVDZ	
Isomer	ΔE_e	ΔE_0	ΔE_e	ΔE_0	ΔE_e	ΔE_0
1	1.20	0.40	0.71	0.41	**0.00**	**0.00**
2	0.85	0.08	1.85	1.36	0.51	0.32
3	1.21	0.19	0.26	0.22	0.13	0.40
4	1.41	0.45	**0.00**	**0.00**	0.18	0.48
5	2.39	1.29	0.97	0.31	1.26	0.91
6	2.26	1.35	1.71	1.72	1.33	1.65
7	**0.00**	**0.00**	6.67	6.21	3.51	3.36

[a] Isomers **3** and **7** were suggested by Douady et al.[40] and Diken et al.,[32] respectively. The boldface energies denote the lowest-lying isomer. The ZPE-corrected relative energies (ΔE_0) at the RIMP2/aVDZ level were obtained using harmonic ZPE estimates at the M06-2X/aVDZ level of theory.

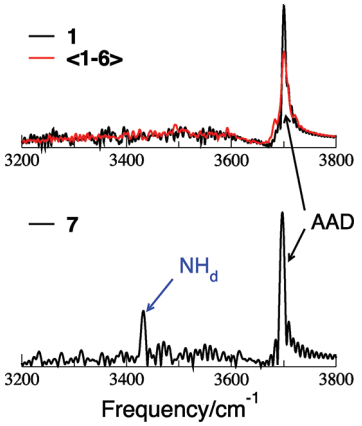

Figure 2. Simulated infrared (IR) spectra of $NH_4^+(H_2O)_{20}$ (frequencies scaled by 1.049). The AAD-type OH_d peak appears at ~3700 cm^{-1}. The AAD-type OH_d peak is from the water molecules on the surface. The cluster **1** and <**1**−**6**> with fully solvated NH_4^+ have no NH_d peak, while the cluster **7** with NH_4^+ on the surface shows the NH_d peak at ~3430 cm^{-1}. Here, <**1**−**6**> indicates the average spectra from six isomers of **1**−**6**.

was added to the RIMP2/aVDZ relative energetics (ΔE_0). The DFT with the B3LYP hybrid functional gave the isomer **7** as the lowest-energy isomer, while M06-2X and RIMP2 gave the highest energy among the given **7** structures (Figure 1). Furthermore, the geometries optimized at B3LYP/aVDZ′ were quite different from those optimized at M06-2X/aVDZ and RIMP2/aVDZ (these optimized geometries are provided in the Supporting Information). In detail, the former prefers to form a four-hydrogen-bond network of NH_4^+ with the pentagonal dodecahedron $(H_2O)_{20}$ cages, while the latter prefers a five- or more hydrogen-bond network. This wide deviation in the relative energies of the B3LYP functional from the RIMP2 level of theory is mainly due to underestimation of the dispersion interaction in DFT.[56−59] Hence, the M06-2X functional with the corrected dispersion interaction gives a highly improved description for both potential energies and geometric features of $NH_4^+(H_2O)_{20}$ clusters. We confirmed that isomer **7** has much higher energy than the solvated NH_4^+ clusters (isomers **1**−**6**) at the level of RIMP2/aVDZ. In order to make sure that isomer **1** is one candidate for the lowest isomer, we performed geometry optimization at the level of RIMP2/aVDZ for the low-lying isomer (isomer **3** in Table 1) suggested by Douady et al.[40] and computed its relative energy of ΔE_e = 0.13 kcal/mol and ΔE_0 = 0.4 kcal/mol. In summary, isomers **1**, **2**, **3**, and **4** with fully solvated NH_4^+ are nearly isoenergetic lowest-energy structures.

Since the simulated vibrational spectra can give insight into the origin of the "no peaks" of NH_d stretching of the vibrational spectra of $NH_4^+(H_2O)_{20}$, we performed Car−Parrinello molecular dynamics (CP-MD) simulations[64,65] at a temperature of 125 K for the seven low-lying isomers shown in Figure 1. Note that the CP-MD IR spectra are more realistic, being closer to the experimental data since the CP-MD IR spectra reflect both the anharmonic potential surfaces and the contribution of temperature. Figure 2 shows the simulated vibrational spectrum in the broad range 3200−3800 cm^{-1} for two isomers **1** and **7**. The dangling AAD-type OH_d peak appears at ~3700 cm^{-1}, indicating that both isomers **1** and **7** have the AAD-type OH_d on the water cages of $NH_4^+(H_2O)_{20}$. Note that the AAD-type OH_d peak from $NH_4^+(H_2O)_{20}$ is also shown in the IR spectra of $H_3^+O(H_2O)_{20}$.[49] Both $NH_4^+(H_2O)_{20}$ and $H_3^+O(H_2O)_{20}$ have the water cage with the dangling OH_d on their cage surface. In comparison with isomer **1**, the additional IR peak near ~3430 cm^{-1} appears in isomer **7**. This additional peak is mainly due to the dangling NH_d stretching of NH_4^+, which was confirmed in the vibrational spectra of smaller clusters of $NH_4^+(H_2O)_n$ ($n < 8$).[34] Hence, the NH_d peak near ~3430 cm^{-1} becomes the unique peak to identify whether NH_4^+ is fully solvated in water clusters. The experimental vibrational spectrum[32] of $NH_4^+(H_2O)_{20}$ did not show the dangling NH_d stretching peak near 3430 cm^{-1}. We suggest that the absence of the experimental peak of NH_d near 3430 cm^{-1} in $NH_4^+(H_2O)_{20}$ indicates clearly that the ammonium cation NH_4^+ is fully solvated in most structures of $NH_4^+(H_2O)_{20}$.

Why is the ammonium cation NH_4^+ fully solvated in $NH_4^+(H_2O)_n$ ($n \geq 6$)? And why can the hydronium cation H_3O^+ not be fully solvated in $H_3O^+(H_2O)_{20}$? All hydrogen atoms of NH_4^+ have a favorable hydrogen bonding interaction with the oxygen atom of a water molecule. Thus, its solubility is similar to that of alkali cations (Na^+, K^+, and Cs^+). In contrast, the oxygen atom of H_3O^+ is hydrophobic, as in our previous work,[68] since it is no longer a good electron donor or proton acceptor for the formation of a hydrogen bonding interaction. Hence, the hydronium shows an amphiphilic behavior. The H_3O^+ ion favors the surface to maximize the polarization-driven binding energy, as shown in amphiphilic species such as lipids. Though the H atoms in H_3O^+ are involved in the H bonding, the O atom is not involved in the H bonding. Thus, the H_3O^+ remains on the surface of the cluster with three H bonds by three H atoms, while there is no H bond by the O atom. On the other hand, the NH_4^+ prefers the internal structure forming a five or more H-bond network with the pentagonal dodecahedron $(H_2O)_{20}$ cages.

In summary, we performed the CP-MD simulations at 125 K in conjunction with DFT calculations to generate the simulated IR spectra of $NH_4^+(H_2O)_{20}$. When the experimental vibrational spectrum of $NH_4^+(H_2O)_{20}$ was compared with those of **1** and **7**, the simulated spectrum of **1** (the isomer with fully solvated NH_4^+) was consistent with the experimental vibrational spectra. This result indicates that in experimentally measured structures of $NH_4^+(H_2O)_{20}$ the ammonium cation NH_4^+ is fully solvated

inside the cage structure of $(H_2O)_{20}$ against *on* the surface structure. Even though the experimental vibrational spectra of $NH_4^+(H_2O)_{20}$ are no different from those of $H_3O^+(H_2O)_{20}$ in the broad range 3200−3800 cm^{-1}, the geometric features of $NH_4^+(H_2O)_{20}$ are very different from those of $H_3O^+(H_2O)_{20}$.

■ ASSOCIATED CONTENT

Supporting Information. Total electronic energies (E_e) and zero-point corrected energies (E_0) and the optimized geometries of low-lying isomers shown in Figure 1. This material is available free of charge via the Internet http://pubs.acs.org.

■ AUTHOR INFORMATION

Corresponding Author

*Tel.: +82-54-279-2110. Fax: +82-54-279-8137. E-mail: kim@postech.ac.kr (K.S.K.), jiten@postech.ac.kr (N.J.S.).

■ ACKNOWLEDGMENT

This work was supported by NRF (National Honor Scientist Program: 2010-0020414, WCU: R32-2008-000-10180-0) and KISTI (KSC-2011-G3-02).

■ REFERENCES

(1) Stace, A. *Science* **2001**, *294*, 1292–1293.
(2) Singh, N. J.; Olleta, A. C.; Kumar, A.; Park, M.; Yi, H.-B.; Bandyopadhyay, I.; Lee, H. M.; Tarakeshwar, P.; Kim, K. S. *Theor. Chem. Acc.* **2005**, *115*, 127–135.
(3) Knipping, E. M.; Lakin, M. J.; Foster, K. L.; Jungwirth, P.; Tobias, D. J.; Gerber, R. B.; Dabdub, D.; Finlayson-Pitts, B. J. *Science* **2000**, *288*, 301–306.
(4) Miller, D. J.; Lisy, J. M. *J. Chem. Phys.* **2006**, *124*, 184301.
(5) Vaden, T. D.; Lisy, J. M.; Carnegie, P. D.; Dinesh Pillai, E.; Duncan, M. A. *Phys. Chem. Chem. Phys.* **2006**, *8*, 3078.
(6) Kolaski, M.; Lee, H. M.; Choi, Y. C.; Kim, K. S.; Tarakeshwar, P.; Miller, D. J.; Lisy, J. M. *J. Chem. Phys.* **2007**, *126*, 074302.
(7) Reinhard, B. M.; Niedner-Schatteburg, G. *Phys. Chem. Chem. Phys.* **2002**, *4*, 1471–1477.
(8) Sobott, F.; Wattenberg, A.; Barth, H.-D.; Brutschy, B. *Int. J. Mass Spectrom.* **1999**, *187*, 271–279.
(9) Lee, H. M.; Min, S. K.; Lee, E. C.; Min, J.-H.; Odde, S.; Kim, K. S. *J. Chem. Phys.* **2005**, *122*, 064314.
(10) Karthikeyan, S.; Park, M.; Shin, I.; Kim, K. S. *J. Phys. Chem. A* **2008**, *112*, 10120–10124.
(11) Lehr, L.; Zanni, M. T.; Frischkorn, C.; Weinkauf, R.; Neumark, D. M. *Science* **1999**, *284*, 635–638.
(12) Robertson, W. H.; Johnson, M. A. *Science* **2002**, *298*, 69–69.
(13) Robertson, W. H.; Diken, E. G.; Price, E. A.; Shin, J.-W.; Johnson, M. A. *Science* **2003**, *299*, 1367–1372.
(14) Hurley, S. M.; Dermota, T. E.; Hydutsky, D. P.; Castleman, A. W., Jr. *Science* **2002**, *298*, 202–204.
(15) Kim, J.; Lee, H.; Suh, S.; Majumdar, D.; Kim, K. S. *J. Chem. Phys.* **2000**, *113*, 5259–5272.
(16) Odde, S.; Mhin, B. J.; Lee, S.; Lee, H. M.; Kim, K. S. *J. Chem. Phys.* **2004**, *120*, 9524.
(17) Wang, X.-B.; Kowalski, K.; Wang, L.-S.; Xantheas, S. S. *J. Chem. Phys.* **2010**, *132*, 124306.
(18) Yates, B. F.; Schaefer, H. F., III; Lee, T. J.; Rice, J. E. *J. Am. Chem. Soc.* **1988**, *110*, 6327–6332.
(19) Kemp, D. D.; Gordon, M. S. *J. Phys. Chem. A* **2005**, *109* 7688–7699.
(20) Gruenloh, C. J.; Carney, J. R.; Arrington, C. A.; Zwier, T. S.; Fredericks, S. Y.; Jordan, K. D. *Science* **1997**, *276*, 1678–1681.
(21) Losada, M.; Leutwyler, S. *J. Chem. Phys.* **2002**, *117*, 2003–2016.
(22) Day, P.; Pachter, R.; Gordon, M. S.; Merrill, G. N. *J. Chem. Phys.* **2000**, *112*, 2063–2073.
(23) Bulusu, S.; Yoo, S.; Aprà, E.; Xantheas, S.; Zeng, X. C. *J. Phys. Chem. A* **2006**, *110*, 11781–11784.
(24) Yoo, S.; Aprà, E.; Zeng, X. C.; Xantheas, S. S. *J. Phys. Chem. Lett.* **2010**, *1*, 3122–3127.
(25) Lagutschenkov, A.; Fanourgakis, G.; Niedner-Schatteburg, G.; Xantheas, S. S. *J. Chem. Phys.* **2005**, *122*, 194310.
(26) Lenz, A.; Ojamäe, L. *J. Phys. Chem. A* **2006**, *110*, 13388–13393.
(27) Lee, H. M.; Suh, S. B.; Lee, J. Y.; Tarakeshwar, P.; Kim, K. S. *J. Chem. Phys.* **2000**, *112*, 9759.
(28) Lee, H.; Suh, S.; Lee, J.; Tarakeshwar, P.; Kim, K. *J. Chem. Phys.* **2001**, *113*, 3343.
(29) Shinohara, H.; Nagashima, U.; Nishi, N. *Chem. Phys. Lett.* **1984**, *111*, 511–513.
(30) Perrin, C. L.; Gipe, R. K. *Science* **1987**, *238*, 1393–1394.
(31) Fox, B. S.; Beyer, M. K.; Bondybey, V. E. *J. Phys. Chem. A* **2001**, *105*, 6386–6392.
(32) Diken, E. G.; Hammer, N. I.; Johnson, M. A.; Christie, R. A.; Jordan, K. D. *J. Chem. Phys.* **2005**, *123*, 164309.
(33) Pankewitz, T.; Lagutschenkov, A.; Niedner-Schatteburg, G.; Xantheas, S. S.; Lee, Y.-T. *J. Chem. Phys.* **2007**, *126*, 074307.
(34) Wang, Y.-S.; Chang, H.-C.; Jiang, J.-C.; Lin, S. H.; Lee, Y. T.; Chang, Y.-T. *J. Am. Chem. Soc.* **1998**, *120*, 8777–8788.
(35) Jiang, J.-C.; Chang, H.-C.; Lee, Y. T.; Lin, S. H. *J. Phys. Chem. A* **1999**, *103*, 3123–3135.
(36) Brugé, F.; Bernasconi, M.; Parrinello, M. *J. Am. Chem. Soc.* **1999**, *121*, 10883–10888.
(37) Chang, T.; Dang, L. X. *J. Chem. Phys.* **2003**, *118*, 8813–8820.
(38) Lee, H. M.; Tarakeshwar, P.; Park, J.; Kołaski, M. R.; Yoon, Y. J.; Yi, H.-B.; Kim, W. Y.; Kim, K. S. *J. Phys. Chem. A* **2004**, *108*, 2949–2958.
(39) Karthikeyan, S.; Singh, J. N.; Park, M.; Kumar, R.; Kim, K. S. *J. Chem. Phys.* **2008**, *128*, 244304.
(40) Douady, J.; Calvo, F.; Spiegelman, F. *J. Chem. Phys.* **2008**, *129*, 154305.
(41) Zhao, Y.-L.; Meot-Ner Mautner, M.; Gonzalez, C. *J. Phys. Chem. A* **2009**, *113*, 2967–2974.
(42) Kim, H.; Lee, H. M. *J. Phys. Chem. A* **2009**, *113*, 6859–6864.
(43) Morrell, T. E.; Shields, G. C. *J. Phys. Chem. A* **2010**, *114*, 4266–4271.
(44) Miyazaki, M.; Fujii, A.; Ebata, T.; Mikami, N. *Science* **2004**, *304*, 1134–1137.
(45) Mizuse, K.; Fujii, A. *J. Phys. Chem. Lett.* **2011**, *2*, 2130–2134.
(46) Shin, J.-W.; Hammer, N. I.; Diken, E. G.; Johnson, M. A.; Walters, R. S.; Jaeger, T. D.; Duncan, M. A.; Christie, R. A.; Jordan, K. D. *Science* **2004**, *304*, 1137–1140.
(47) Wu, C.-C.; Lin, C.-K.; Chang, H.-C.; Jiang, J.-C.; Kuo, J.-L.; Klein, M. L. *J. Chem. Phys.* **2005**, *122*, 074315.
(48) Iyengar, S. S.; Petersen, M. K.; Day, T. J. F.; Burnham, C. J.; Teige, V. E.; Voth, G. A. *J. Chem. Phys.* **2005**, *123*, 084309.
(49) Singh, N. J.; Park, M.; Min, S. K.; Suh, S. B.; Kim, K. S. *Angew. Chem., Int. Ed.* **2006**, *118*, 3879–3884.
(50) Elstner, M.; Porezag, D.; Jungnickel, G.; Elsner, J.; Haugk, M.; Frauenheim, T.; Suhai, S.; Seifert, G. *Phys. Rev. B* **1998**, *58*, 7260–7268.
(51) Li, Z.; Scheraga, H. A. *Proc. Natl. Acad. Sci. U.S.A.* **1987**, *84*, 6611–6615.
(52) Wales, D.; Hodges, M. P. *Chem. Phys. Lett.* **1998**, *286*, 65–72.
(53) Becke, A. D. *Phys. Rev. A* **1988**, *38*, 3098–3100.
(54) Lee, C.; Yang, W.; Parr, R. *Phys. Rev. B* **1988**, *37*, 785–789.
(55) Weigend, F.; Haser, M.; Patzelt, H.; Ahlrichs, R. *Chem. Phys. Lett.* **1998**, *294*, 143–152.
(56) Grimme, S.; Antony, J.; Schwabe, T.; Mck-Lichtenfeld, C. *Org. Biomol. Chem.* **2007**, *5*, 741.
(57) Gräfenstein, J.; Cremer, D. *J. Chem. Phys.* **2009**, *130*, 124105.
(58) Johnson, E. R.; Mackie, I. D.; DiLabio, G. A. *J. Phys. Org. Chem.* **2009**, *22*, 1127–1135.
(59) Zhao, Y.; Truhlar, D. G. *Theor. Chem. Acc.* **2007**, *120*, 215–241.

(60) Dunning, T., Jr. *J. Chem. Phys.* **1989**, *90*, 1007–1023.
(61) Kendall, R.; Dunning, T., Jr.; Harrison, R. *J. Chem. Phys.* **1992**, *96*, 6796–6806.
(62) Frisch, M. J.; Trucks, G. W.; Schlegel, H. B.; Scuseria, G. E.; Robb, M. A.; Cheeseman, J. R.; Montgomery, J. A., Jr.; Vreven, T.; Kudin, K. N.; Burant, J. C.; Millam, J. M.; Iyengar, S. S.; Tomasi, J.; Barone, V.; Mennucci, B.; Cossi, M.; Scalmani, G.; Rega, N.; Petersson, G. A.; Nakatsuji, H.; Hada, M.; Ehara, M.; Toyota, K.; Fukuda, R.; Hasegawa, J.; Ishida, M.; Nakajima, T.; Honda, Y.; Kitao, O.; Nakai, H.; Klene, M.; Li, X.; Knox, J. E.; Hratchian, H. P.; Cross, J. B.; Bakken, V.; Adamo, C.; Jaramillo, J.; Gomperts, R.; Stratmann, R. E.; Yazyev, O.; Austin, A. J.; Cammi, R.; Pomelli, C.; Ochterski, J. W.; Ayala, P. Y.; Morokuma, K.; Voth, G. A.; Salvador, P.; Dannenberg, J. J.; Zakrzewski, V. G.; Dapprich, S.; Daniels, A. D.; Strain, M. C.; Farkas, O.; Malick, D. K.; Rabuck, A. D.; Raghavachari, K.; Foresman, J. B.; Ortiz, J. V.; Cui, Q.; Baboul, A. G.; Clifford, S.; Cioslowski, J.; Stefanov, B. B.; Liu, G.; Liashenko, A.; Piskorz, P.; Komaromi, I.; Martin, R. L.; Fox, D. J.; Keith, T.; Al-Laham, M. A.; Peng, C. Y.; Nanayakkara, A.; Challacombe, M.; Gill, P. M. W.; Johnson, B.; Chen, W.; Wong, M. W.; Gonzalez, C.; Pople, J. A. *Gaussian 03*, Revision C.02; Gaussian, Inc.: Wallingford, CT, 2004.
(63) Ahlrichs, R.; Bar, M.; Haser, M.; Horn, H.; Kolmel, C. *Chem. Phys. Lett.* **1989**, *162*, 165−169. {Available from TURBOMOLE-Program Package for ab initio Electronic Structure Calculations. http://www.turbomole.com (accessed Sep 27, 2011).}
(64) Car, R.; Parrinello, M. *Phys. Rev. Lett.* **1985**, *55*, 2471–2474.
(65) *CPMD*; IBM Corp.: Armonk, NY, 1990; MPI für Festkörperforschung Stuttgart: Stuttgart, Germany, 1997. http://www.cpmd.org/ (accessed Sep 27, 2011).
(66) Troullier, N.; Martins, J. *Phys. Rev. B* **1991**, *43*, 1993–2006.
(67) Schmitt, U. W.; Voth, G. A. J. *Chem. Phys.* **1999**, *111*, 9361.
(68) Park, M.; Shin, I.; Singh, N. J.; Kim, K. S. J. *Phys. Chem. A* **2007**, *111*, 10692–10702.